Journal of Materials Science and Nanotechnology
Volume 12 | Issue 1
ISSN: 2348-9812

Research Article Open Access

Investigation of the Characteristics and Performance of Compatibilized PLA/P-CL Blends and Their Nanocomposites with Nanocalcium Carbonate

Mohammadmahdi Negaresh[1,*], Azizeh Javadi[1] and Hamid Garmabi[1]

Department of Polymer Engineering and Color Technology, Amirkabir University of Technology, Tehran, Iran

***Corresponding Author:** Mohammadmahdi Negaresh, Department of Polymer Engineering and Color Technology, Amirkabir University of Technology, Tehran, Iran, Tel.: 09124800598, E-mail: m_neg112@aut.ac.ir

Citation: Mohammadmahdi Negaresh, Azizeh Javadi, Hamid Garmabi (2024) Investigation of the Characteristics and Performance of Compatibilized PLA/PCL Blends and Their Nanocomposites with Nanocalcium Carbonate, J Mater Sci Nanotech nol 12(1): 105

Received Date: June 03, 2024 **Accepted Date:** July 03, 2024 **Published Date:** July 07, 2024

Abstract

In this research, (Poly lactic acid)(PLA)/Poly(ε-caprolactone)(PCL) blends containing 2 and 3 phr glycidyl methacrylate (GMA) as a chain extender, and nanocomposites of compatibilized and uncompatibilized PLA/PCL containing 7 and 9 phr nanocalcium carbonate (NCC) were prepared via melt mixing. The crystallinity, tensile properties, morphology, permeability and rheology of the samples were investigated. The results showed that using 25 wt. % of PCL leads to optimum properties of PLA/PCL blends. The crystallinity of this sample was increased from 5 (for neat PLA) to 27% in the sample containing both GMA and NCC. In addition, the elongation at break of the compatibilized blend is improved up to 180% in comparison to neat PLA. The result showed that the barrier properties of PLA/PCL blends were increased by the crystallinity enhancement of PLA and the intrinsic low permeability of PCL. It was found that the addition of 9 phr NCC to this sample promotes crystallinity and barrier properties, but causes lower tensile properties of blends. Finally, the use of NCC and GMA simultaneously results in lower crystallinity and barrier properties, which could be due to the phase separation of components in the blends. The barrier properties of some samples like compatibilized nanocomposite in composition of 9 phr NCC are closer to PE and PP and thus suitable for replacing of oil based polymers.

Keywords: Biopolymers; polymer blends; nanocomposites; oxygen permeability; packaging

Introduction

The reduction of packaging wastes and the consumption of non-renewable resources have been strong motivations for replacing the most common plastics with biodegradable materials. So nowadays, many researchers attempt to find suitable biopolymers with low cost and easy processing technology [1].

One of the best choices for replacing biodegradable polymers with non-biodegradable is PLA. PLA has good strength and process ability, but this biopolymer also has some weaknesses such as low toughness and barrier properties [2], which lead to reducing in the usage of PLA in different applications like packaging. Some of these weaknesses could be improved by blending PLA with other polymers or adding some nanoparticles [3]. The PLA properties depend on the ratio between the two enantiomers D-lactic acid and L-lactic acid. However, to further improvement of some properties such as impact strength, PLLA blends with more flexible polymers such as PCL have been developed [4]. Considerable academic and industrial efforts have been focused on PLA modification for extending its applications in the food packaging industry, such as the addition of modifiers, nanotechnology, copolymerization or blending. It is known that the increase of crystallinity level, could improve the use of PLA as food packaging material, due to its direct impact on gas permeation. Melt blending of PLA with some more crystalline and low permeable biopolymers like poly (ε-caprolactone) (PCL), has gained considerable attention for applications in food packaging. Many studies showed that the morphology of PLA/PCL blends depend on the molecular weight of PLA and PCL. It was shown that the high molecular weight PCL is not miscible with PLA, and in order to achieve a PLA/PCL blend with good properties, a suitable compatibilizer should be used. Many compatibilizers such as acetyl tributyl citrate (ATBC), poly (ethylene glycol)(PEG), poly (vinyl acetate)(PVAc) and also some nanoparticles have been used in PLA/PCL blends to compatibilize the PLA and PCL phases[5].

Blending PLA and PCL presents a range of challenges and limitations in practical applications. The limited mechanical properties of both polymers, with PLA being brittle and PCL being soft, may result in a blend with compromised properties such as reduced tensile strength and increased ductility. Additionally, the different melt temperatures and viscosities of PLA and PCL can lead to processing difficulties, resulting in inconsistent material properties and difficulties in shaping the blend into complex forms. While blending may improve thermal stability and biodegradability, limitations in high-temperature applications and control over degradation rates may arise. Furthermore, the higher production costs and limited compatibility with other materials may also restrict the suitability of the blend for certain applications. Overall, careful consideration of desired properties and processing conditions is essential to maximize the potential benefits of blending PLA and PCL in various applications [6].

Blends of PLA/PCL have good barrier properties, but very low flexibility. In some recent researches, in order to boost the flexibility of this blend, plasticized PLA/PCL containing low molecular weight plasticizers like glycidyl methacrylate (GMA), are attended. GMA is able to improve the elongation at break and flexibility of this blend. GMA has many advantages in comparison to the other chain extenders, as its reasonable boiling point, which makes it suitable for melt blending. Arrieta et al. [7] showed that PLA/PCL blends have high thermal stability in the presence of GMA in comparison to other plasticizers like PEG. GMA also shows a solubility parameter close to PLA and PCL values. Solubility parameters of PLA and PCL are (19.5-20.5) and (18.5-20.1) $MPa^{0.5}$, respectively [8]. This is another advantage of the GMA plasticizer for use in the PLA/PCL system.

On the other hand, different nanoparticles have been used for improving mechanical and barrier properties, and also improving the compatibility between polymers in blends [9]. One of the efficient nanoparticles to improve the barrier properties of polymers is nanocalcium carbonate (NCC). This nanoparticle has a spherical structure, so it can be an obstacle for gas transmission throughout polymers, and therefore improves the barrier properties, which is very important especially in food packaging. Up to now, different NCC have been added to PLA or PCL matrices, and it is shown that it is more suitable for PLA/PCL blends. It is reported that the greater decrease in the oxygen permeability of PLA occurs using this nanoparticle [10].

The research group conducted a study on the mentioned blend in their previous work, investigating both the individual components of compatibilizers and nanoparticles [11]. The study involved determining the optimal combination of percentages of these two components to analyze their presence in the blend. In this research, the effect of simultaneous presence of GMA, NCC, were investigated on the flexibility and barrier properties of PLA/PCL blends. The crystallinity and morphology of blends and nanocomposites were also studied.

Experimental

Materials

Poly (lactic acid) (PLA) with a grade of 2003D, obtained from Nature Works, USA, has a melt flow rate of 6 g/10 min (190° C/2.16 kg) and a density of 1.24 g/cm^3. The Poly (ε-caprolactone) (PCL) used is Capa^{TM}6800, purchased from Perstorp, Sweden, with a melt flow rate of 4 g/10 min (160° C/5 kg) and a density of 1.13 g/cm^3. Glycidyl methacrylate (GMA), obtained from Alfa Aesar, Germany, has a density of 1.08 g/cm^3 and a boiling point of 189° C. Nano calcium carbonate (NCC) with a mean particle diameter of 80 nm and a density of 2.65 g/cm^3 was purchased from Shiraishi (Austria) and treated with stearic acid.

Samples Preparation

To prepare materials for compounding, they were dried in a vacuum oven at 70° C for 16 hours. The compounding process was performed using an internal mixer (Brabender Plasticorder W50) with a capacity of 60 cm^3. The components were mixed simultaneously at 170° C and 50 rpm for 10 minutes. The resulting mixture was then compression molded at 190° C to form sheets of 2 and 3 mm thickness for subsequent measurements.

For the sample preparation, three steps were taken:

Simple blend of PLA/PCL with 25 wt.% of PCL was prepared as a basic sample to study properties considered.

Compatibilized PLA/PCL (75/25) blend with 2 and 3 phr of GMA compatibilizer were prepared and their properties were studied.

PLA/PCL nanocomposites with different amounts of NCC (7 and 9 phr) were made and their properties were investigated as well.

The Table 1 provides a summary of the names and compositions of the neat polymers, blends, and nanocomposites. For instance, P75G2 represents a nanocomposite sample containing 75 wt.% of PLA, 25 wt.% of PCL, and 2 phr of GMA.

Table 1: Summarized name and composition of prepared samples

Samples	PLA(wt.%)	PCL(wt.%)	NCC(phr)	GMA(phr)
P100	100	0	0	0
C100	0	100	0	0
P75	75	25	0	0
P75G2	75	25	0	2
P75G3	75	25	0	3
P75N7	75	25	7	0
P75N9	75	25	9	0

P75G2N7	75	25	2	7
P75G3N11	75	25	3	9

Characterization

Mechanical Characterization

Tensile tests were conducted using a SUN 2500, Galdabini universal testing machine according to ASTM D638 with a strain rate of 5 mm/min at ambient temperature. Five dumbbell-shaped specimens with a thickness of 2 mm were tested for each sample, and the mean values were reported.

Differential Scanning Calorimetry (DSC)

Nonisothermal crystallization behavior of the samples was determined using a DSC1, Mettler Toledo differential scanning calorimeter. The samples were heated from room temperature to 200° C at a rate of 10° C/min and held at this temperature for 5 minutes to eliminate thermal history. Subsequently, the samples were cooled to room temperature at the same rate and then heated to 200° C at a rate of 10° C/min again.

The crystallinity of the samples was calculated using the cooling process, and melting behavior was assessed through the second heating process. The crystallinity (X_c) was calculated according to Equation (1) [12].

$$X_c(\%) = \left(\frac{\Delta H_m - \Delta H_{CC}}{\Delta H_m^0 \left(\frac{\varphi_{PLA}}{100}\right)}\right) \times 100 \quad (1)$$

In this Equation, ΔH_m and ΔH_{cc} refer to the melting and cold crystallization enthalpy of the samples respectively, determined from the DSC thermogram. ϕ_{PLA} represents the weight percentage of PLA in the blends, and ${}_i ny \Delta H_m^0$ presents the enthalpy of 100% crystalline PLA (93.6 J/g) [12].

Morphology

The morphology of the blends was examined using a scanning electron microscope (SEM) (DSM 960 A, Germany) operated at 10 kV accelerating voltage. The samples were cryogenically fractured after being stored in liquid nitrogen for 15 minutes. The fracture surface of the samples was coated with gold using a sputter coater to enhance conductivity.

Oxygen Transmission Rate (OTR)

The measurements were carried out using an oxygen permeation analyzer (Tarbiat Modaress University, Tehran).

X-Ray Diffraction (XRD)

This test was performed using an Xpert-Pro power x-ray diffractometer. Scans were carried out on PLA/PCL/NCC composites. All measurements were run from 1˚ to 40˚ at a step size of 0.02˚. The interlayer spacing of NCC particles was calculated using Equation (2) [12].

$$d = \frac{n\lambda}{2\sin\theta} (2)$$

Where n is an integer (in this case 1), λ is the wavelength of x-rays (in this case 1.54 A°); d is interlayer spacing and θ is the diffraction angle.

Scanning Electron Microscopy (SEM)

The samples were fractured in liquid nitrogen, then coated with gold-palladium prior to scanning. Then the specimens were viewed using a DSM 960A Germany field emission scanning electron microscope at 10 KV. The size of the dispersed phase was determined using Image J software.

Atomic Force Microscope (AFM)

The images were captured using a DME atomic force microscope with a dual-scope C-26 controller. The test was conducted at room temperature under non-contact mode using a 95- 200E scanner. The silicon probe had a tip radius of approximately 15 nm. The surfaces of the samples were scanned without any image processing.

Rheology

A rheo mechanical spectroscopy (RMS) apparatus, specifically the Anton-Paar 302 model, with parallel plates set at 1 mm distance with a diameter of 25 mm operating at 180° C, was used to study the small amplitude oscillatory shear rheology (SAOS) of the unblended individual polymers, including neat samples, blends with and without compatibilizer, and nanocomposite blends.

Dynamic Mechanical Analysis (DMA)

This test was conducted using a dynamic mechanical analyzer (MK11, Polymer Laboratory). The storage modulus was tested at a fixed frequency of 1 Hz, with a dynamic strain of 0.025%, and temperature ranging from 60 to 180° C. The scanning rate was set at 2 °C/min.

Dynamic Light Scattering (DLS)

The technique was employed to determine the hydrodynamic diameter of particles. Analysis of the particle size of the NCC particles sample was conducted using the Litesizer™ 500 instrument, with measurements performed under specific conditions including a wavelength of 658 nm, particle absorption coefficient of 0.01, diffusion coefficient of 6.2 $\mu m^2/s$, water refractive index of 1.33, and intensity of 79.67 nm. For particle size measurement, 0.1 ml of the NCC solution in 2 ml of deionized water (DI H_2O) was placed in a polystyrene cuvette and analyzed at the temperature of 25°C.

Results and Discussion

Mechanical Properties

Tensile properties and impact strengths are presented in Table 2 and reveal that incorporating ductile PCL into PLA improved its toughness. Brittle fracture observed in neat PLA indicated a lack of yield phenomenon. However, the presence of PCL introduced a shear yielding mechanism that enhanced the toughness of PLA. Interestingly, the sample containing 25 wt.% of PCL exhibited literally high elongation at break. This behavior is likely attributed to phase separation between PLA and PCL at higher PCL loadings, resulting in poor interfacial adhesion, as supported by previous studies [13]. The PLA/PCL blend demonstrates a lower critical solution temperature (LCST), in which the optimum PCL composition for the initiation of phase separation was estimated to be around 36% by volume. Consequently, the PLA/PCL blend with a ratio of 75/25 was selected for further experimentation.

To improve compatibility of PLA and PCL, GMA was employed as a reactive compatibilizer in the blend. Notably, the addition of 2 and 3 phr of GMA to P75 increased the elongation at break. This improvement can be attributed to enhanced miscibility

between PLA and PCL, as well as the uniform distribution of PCL droplets facilitated by GMA because of the reduction of interfacial tension. The positive impact of GMA on the mechanical properties of polymer blends has been reported previously [14]. The results presented in Table 2 reveal that increasing content of GMA to 3 phr further improves the elongation at break and impact strength of the samples. However, it seems that exceeding the optimum amount of compatibilizer (3 phr) had an adverse effect on the mechanical properties, potentially due to phase separation. This behavior signifies that an extra quantity of compatibilizer within the blend did not undergo any reaction; therefore, its influence on softening of polymer phases decreased the mechanical properties. In the regions where this unreacted compatibilizer existed, the movement of polymer chains accelerated, as the induced free volume within the system increased. Moreover, a significant rise in elongation at break of polymer blends is attributed to the lubricating effect of GMA, and thus improved fluidity of molecular chain.

In a previous paper, incorporating more than 3 wt.% of GMA into PLA/PCL blends resulted in a decrease in flexural modulus, elongation at break, and impact strength. Also, Zhang et al. [15] found that increasing the T-GMA content initially improved the elongation at break, but subsequent increases ultimately reduced this property.

Table 2: Mechanical properties of neat PLA and PCL and their blends and nanocomposites

Samples	Tensile Modulus(MPa)	Tensile Strength(MPa)	Elongation at Break (%)
P100	2134±84	59.5±2.4	7.5±0.9
C100	286±12	21.2±1.4	>560
P75	1796±73	43.5±1.3	35.1±1.5
P75G2	1722±68	44.8±0.6	92.3±6.1
P75G3	1646±64	42.1±1.2	130.5±8.9
P75N7	2806±103	35.9±1.8	3.8±0.5
P75N9	3222±149	35.2±0.9	3.1±0.6
P75G2N7	3007±162	31.2±1.3	2.1±0.3
P75G3N9	3395±153	33.4±1.1	2.9±0.55

In addition to investigating the effect of NCC on PLA/PCL blends, the impact of different amounts of NCC on uncompatibilized PLA/PCL (75/25) blend was examined. A decrease in tensile strength and elongation at break was seen as the quantity of NCC increased; however, the tensile modulus and impact strength of the samples were increased. The decline in tensile properties can be attributed to reduce chain mobility and the formation of voids during the tensile test, which arose from the discontinuity in load transfer across the chains.

As can be seen in Figure 1, the concurrent presence of both GMA and NCC significantly increased the brittleness of the blend. This can be primarily correlated to the formation of nanoparticle aggregates throughout the sample, whereas previously, most nanoparticles were located at the interface of PLA and PCL. However, the introduction of the GMA altered the interfacial tension of the polymers, preventing the nanoparticles from thermodynamically congregating at the interface. Consequently, to minimize energy levels, the nanoparticles were now more likely to aggregate, leading to the formation of larger, more random structures within the P75G3N9.

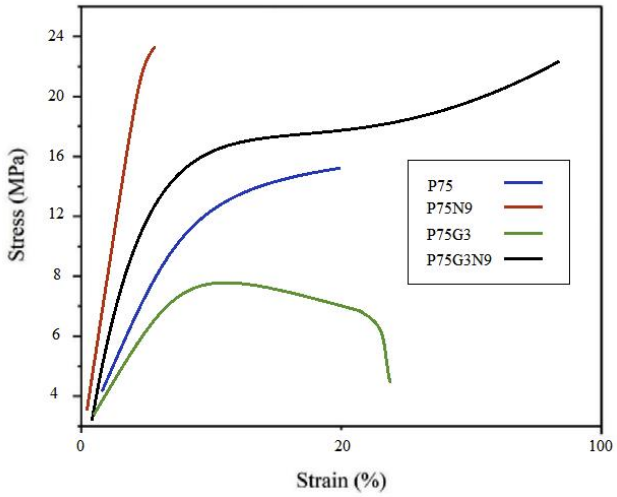

Figure 1: Stress-strain of plots of PLA/PCL, compatibilized and uncompatibilized PLA/PCL (75/25) blends and nanocomposites

Thermal Properties

The glass transition temperature (T_g) can be used to assess miscibility of polymer blend components. A single T_g indicates a blend that is a single phase. Additionally, variations in cold crystallization temperature (T_{cc}), melting temperature (T_m), and percentage of crystallinity (X_C) are often indicative of the interactions between different components. The obtained DSC results are summarized in Table 3 and selected thermographs are shown in Figure 2. To ensure accurate assessments, the thermal data was analyzed based on the second heating run, which eliminates any potential influence of process history.

Table 3: Thermal properties of neat PLA and PCL and their blends and nanocomposites on the second heating run

Samples	T_g (°C)	T_{cc} (°C)	T_m (°C)	ΔH_{cc}(J/g)	ΔH_m (J/g)	X_c(%)
P100	62.4	132	157.6	15.01	16.22	1.3
C100	-	-	55.2	-	-	-
P75	57.1	129.2	153.4	16.49	17.54	1.72
P75G2	55.9	128.2	152.6	16.95	18.42	2.12
P75G3	56.3	127.5	152.1	17.19	18.8	2.34
P75N7	59.6	126.6	157.2	19.57	22.96	4.89
P75N9	60.9	125.8	152.6158.9	19.84	23.74	5.65
P75G2N7	59.1	112.5	151.4159.7	18.22	21.87	3.14
P75G3N9	61.4	120.0	153.7161.9	19.93	23.07	3.45

The neat PLA demonstrates an orthorhombic structure with a crystallization peak at T_c = 132° C and a melting peak at T_m = 157.6° C. On the other hand, neat PCL only exhibits a melting peak at T_m = 55.2° C. P75 blend exhibits lower degree of immiscibility between PLA and PCL among other blend samples. For samples without NCC or GMA, T_{cc} values for all blends are lower than that of neat PLA, with the P75 blend having the lowest value, suggesting the nucleation effect of PCL. Therefore, the P75 sample composition is selected for subsequent samples.

The impact of varying amounts of GMA compatibilizer on the thermal properties of P75 blend was investigated. GMA decreases the T_g and T_m of P75 due to an increase in polymer chain mobility. This is attributed to the reactive epoxide group present in GMA, which can react with both PLA and PCL, facilitating the creation of covalent bonds that bridge the two polymer phases. Consequently, this covalent bonding strengthens the interfacial adhesion and promotes efficient stress transfer between the polymers, resulting in improved chain mobility [16]. Additionally, as the T_g of GMA is lower than both PLA and PCL, its incorporation into the blend leads to an overall reduction in the blend's T_g. This decrease in T_g enhances chain mobility, enabling polymer chain rearrangement and reducing chain entanglements.

In addition, the cold crystallization of PLA in the blend was accelerated after addition of GMA as evidenced by a decrease in T_{cc} and an increase in ΔH_m, in agreement with the findings of Sugih et al. [17]. GMA reduces the size and increases the number of PCL domains and the total area of PLA/PCL interface increases. As a result, the greater the number of PCL domains, the more effective it is as a nucleation agent. In addition, the acceptable effect of GMA on thermal properties of blends took place in the sample containing 3 phr of GMA. The limited interaction capacity between the polymer and compatibilizer led to unreacted GMA, resulting in immiscibility in the P75G4 sample.

Furthermore, the addition of NCC to the P75 increased the T_g and T_m. The T_{cc} of P75 decreased significantly, indicating that NCC enhances the rate of PLA crystallization. This can be attributed to the nucleating effect of the nanoparticle. NCC in 9 phr enhanced thermal properties, as evidenced by a distinct increase in the percentage of crystallinity compared to P75 [18]. Besides T_{cc} changes, it was understood that the P75N9 and P75N11 samples exhibit two distinct melting peaks. According to Figure 2d, low temperature melting peak (T_{m1}) should be associated with the fusion of the crystals grown by normal primary crystallization, whereas the high-temperature melting peak (T_{m2}) is related to the melting peak of the most perfect crystals after rearrangement during the second heating process. This phenomenon happened because of the increment in NCC composition, which prompted reduction of chain mobility and prevented the lamellas from being completed. Therefore, some imperfect crystals with lower lamella's thickness are formed; consequently, double peaks for T_m are seen. Moreover, it is found that the use of 11 phr of NCC in the P75N11 did not make favorable changes in T_{cc} and X_c compared to the P75N9. It seems that the nucleating effect of NCC is restricted due to nanoparticle aggregation. It is important to take into consideration that the process of crystallization is divided into two stages: nucleation and growth of lamellas. The addition of both NCC and GMA enhances nucleation, but the effectiveness of NCC is superior. However, NCC hinders the growth of lamellas by restricting molecular chain movement and resulting in the formation of imperfect lamellas. On the other hand, GMA increases chain mobility and facilitates the arrangement of chains within the lamellas. Therefore, GMA counteracts the formation of imperfect crystals and alters the characteristics of the samples at their melting point.

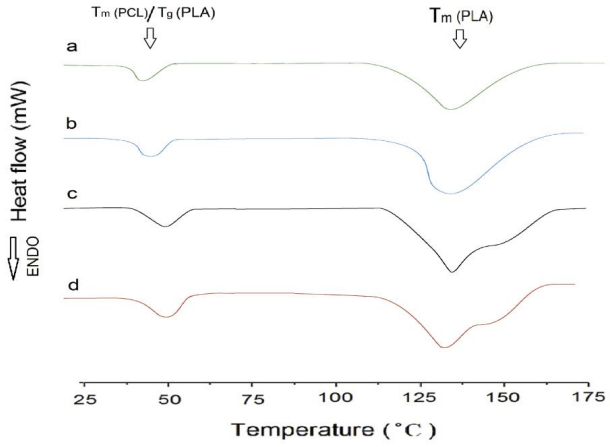

Figure 2: The second heating DSC curves of superior samples in each category:

a) P75, b) P75G3, c) P75N9, and d) P75G3N9

Upon examination of the thermal properties, it is evident that the inclusion of both compatibilizers and nanoparticles in the sample graph results in unique changes. Clumping formations within the blend led to a reduced mobility of the bulk chains and decreased mobility of chains surrounding the nanoparticles, consequently elevating the glass transition temperature. Moreover, the rise in melting temperature and increased crystallinity of the sample suggest a higher concentration of crystalline cells and immobilized chains. These factors collectively contribute to the shift of these characteristics towards higher temperatures. Additionally, the presence of two distinct peaks in the peak analysis further emphasizes the complex nature of these thermal property alterations.

Morphology

The morphology of P75, P70G3, P75N9 and P75G3N9 samples was studied using scanning electron microscopy, and the fracture surfaces images of samples are shown in Figure 3. Images demonstrate that using GMA leads to tough fracture of PLA/PCL blends (Figure 3- B). It is mentioned that the PLA/PCL blends show a brittle fracture, according to SEM images in Arrieta et al. work [19].

As it is observed, the blends have a matrix-dispersed structure. The size of the PCL dispersed phase, which was measured by image j software, is summarized in Table 4.

It is shown that the average size of PCL particles in the P75G3 sample is less than P75. Zhang et al. [20] showed that the presence of amorphous PLA significantly leads to a decrease in the size of PCL spherulites, and this decrease is much more in the samples containing more than 50 wt. % of PLA. They mentioned that the PCL spherulites are very small and well-dispersed in the continuous amorphous PLA phase. Thus, the PCL phase behaves like filler particles for the PLA matrix and improves the mechanical properties of PLA.

In addition, it is observed that the presence of nanocalcium carbonate particles, leads to a decrease in the size of PCL dispersed phases, so it can be concluded that the NCC improves the interaction between PLA and PCL, but increasing the amount of NCC to 9 wt. % diminishes the phase separation of the compatibilizer and two polymers. However, NCC enhanced the interaction between two polymers if it locates at the interface of blends.

Table 4: Average diameters of PCL dispersed phase in PLA matrix

Sample	Phase diameter (μ)
P75	15
P75G3	10
P75N9	22
P75G3N11	17

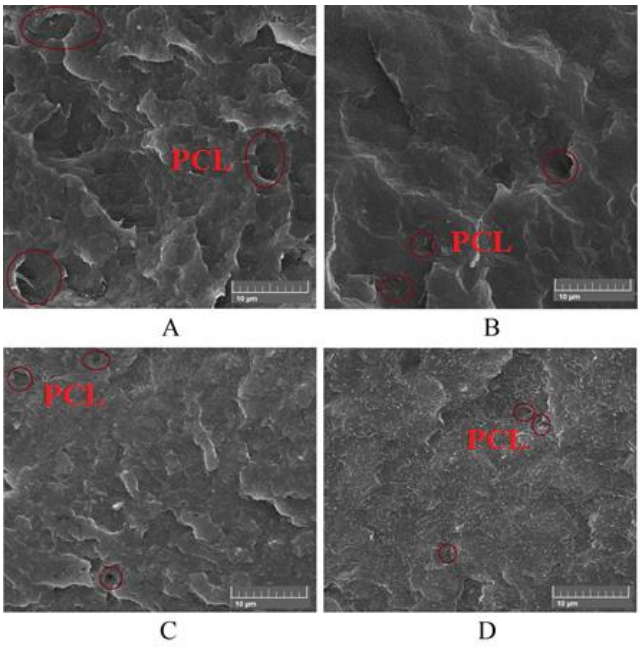

Figure 3: Microstructure of fracture surface: A) P75, B) P75G3, C) P75N9, and D) P75G3N9

Surface Physical Properties

In the subsequent phase of the study, the objective was to analyze the impact of the presence of a compatibilizer on the dispersion efficiency of nanoparticles. Two methods, labeled as SEM and AFM, were implemented for visual observation of any alterations. As illustrated in Figure 4, the presence of the compatibilizer resulted in an enhancement of the compatibility between the two polymer phases. However, due to the reduction in interfacial tension within the blend components, the preferential localization of NCC at the interface was compromised, leading to the formation of nanoparticle aggregartes in both polymers with a wide range of sizes [20]. Consequently, the coexistence of NCC and GMA in the blend is anticipated to diminish its overall properties.

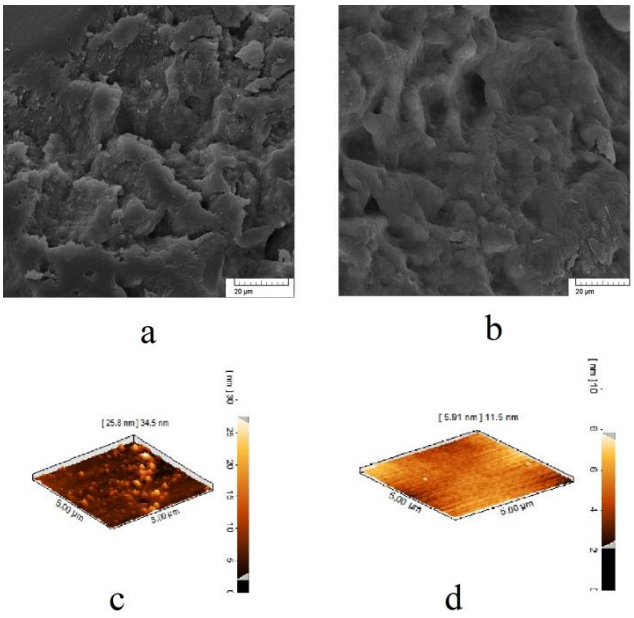

Figure 4: The comparison of the state of distribution of nanoparticles: SEM micrograph of a) P75N9, b) P75G3N9, AFM micrograph of c) P75N9, d) P75G3N9

XRD Analysis

The crystalline structure of the P75, P75N9 and P75G3N9 films were investigated by X-ray diffraction (Figure 5). The peaks of crystals are displayed at 2θ=16.5° for PLA, also at 2θ=13° and 17° for PCL. It is seen that the peak, which was located at 17° overlaps with 16.5°, and cannot clearly be observed in all samples. This is in accordance to Abdelwahab et al. [21] observation. In all three mentioned samples, the peaks of PCL crystals (located at 13°) show a similar intensity in comparison to neat PCL, therefore PLA and NCC do not prevent the crystallization of PCL.

XRD analysis is also used to investigate PLA/PCL/NCC aggregation. Figure 5 shows that the peak of pure NCC exists at 2θ=5.3°, which corresponds to d= 18.5 A°. These values are similar to those reported in the literature [22]. Moreover, it is seen that the incorporation of plasticizer in the PLA/PCL blends leads to an increase in the distance between NCC particles and eases their dispersion. In both samples (P75N9 and P75G3N9), the peak of NCC is changed from 2θ=5.3° to 2.6° (d= 18.5 A° to 33A°). This observation confirms the perfect dispersion of NCC particles in the absence of GMA.

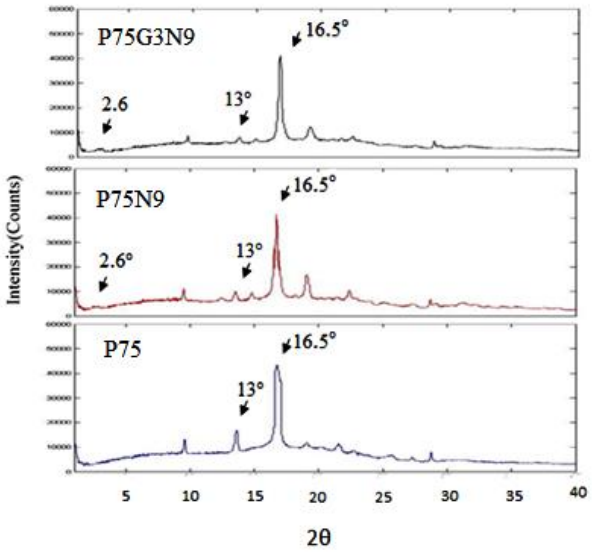

Figure 5: Small angle X-ray diffraction profiles of PLA/PCL blends, compatibilized, and uncompatibilized nanocomposites

Oxygen Permeability

PCL intrinsic oxygen permeability is less than PLA, and the permeability of PLA is decreased by PCL blending. In addition, the crystallinity of PLA is increased in the presence of PCL. This is also observed in previous studies by Arrieta et al. [23]. On the other hand, the addition of GMA leads to increase in the free volume of polymers and higher oxygen permeability once more. For instance, PLA with 3 phr GMA shows an oxygen permeability of 82.3 $_{i}ny\frac{((cm^3mm)}{(m^2dayatm))}$, which is similar to those reported in the literature [24]. The use of the GMA in the samples results in increasing PLA/PCL oxygen permeability. Compatibilized PLA/PCL and their nanocomposites show less oxygen permeability than PLA. Therefore, PCL and NCC were able to decrease PLA permeability in this work.

The addition of 9 phr NCC particles decreased the plasticized PLA/PCL permeability, but in the presence of GMA, the increase of permeability was unexpectedly observed (Table 5). It seems that the permeability, as well as mechanical properties is affected by the phase separation between GMA and polymer phases in the presence of NCC. Thus, the incorporation of nanoparticles suppresses the permeability, due to the spherical structure of this nanoparticle. The permeability is enhanced because of the enlargement of phase separation. Therefore, these two factors compete in the presence of NCC. Finally it is found that all samples

have lower Permeability and higher flexibility compared to the other ordinary food packaging films (like LDPE or PVC) [24].

Table 5: Oxygen permeability results for PLA, PCL, compatibilized PLA/PCL blends and nanocomposites

Samples	OTR
PLA	46.03
P75	72.45
P75G3	68.63
P7N9	74.73
P75G2N7	63.97
P75G3N9	60.06
PCL	28.17

Rheology

Understanding the microstructure of blends and nanocomposites is essential for their characterization, with rheology being a primary method to achieve this. The viscoelastic properties of polymer compounds in a molten state heavily rely on the distribution of nanoparticles and the interaction between fillers and the matrix. Figure 6 illustrates how the storage modulus, loss modulus, and complex viscosity of PLA/PCL (75/25) compatibilized and uncompatibilized nanocomposites vary with different amounts of NCC and GMA.

Analyzing Figure 6a reveals that the storage modulus of PLA is consistently higher than that of PCL across all frequencies. The rheological behavior of the PLA/PCL blend closely resembles that of PLA, indicating that the high modulus of PLA stiffens the blend and restrains the movement of flexible PCL chains. The addition of NCC leads to an increase in storage modulus, loss modulus, and complex viscosity in all frequency ranges, enhancing the overall viscoelastic response compared to pure P75.

The strong interactions between polymer chains and NCC, facilitated by the uniform distribution and high aspect ratio of nanoparticles, play a crucial role in enhancing the storage and loss moduli. The presence of nanoparticles between polymer chains restricts chain mobility and flexibility, resulting in a solid-like behavior. As NCC loading increases, the influence of frequency on storage and loss moduli diminishes, suggesting the formation of nanoparticles-polymer networks that further solidify the composite.

Furthermore, the incorporation of compatibilizers has significantly enhanced the miscibility of the polymer component. The reinforcement of the interface through the formation of hydrogen bonds has resulted in an increase in the blend's brittleness, thereby making the elastic response of the dispersed phase more prominent. Conversely, the concurrent use of nanoparticles and compatibilizers had a detrimental impact on the dispersion of nanoparticles. The presence of GMA at the interface of two polymers has led to the formation of strong bonds in these regions, causing a reduction in interfacial tension and consequently decreasing the likelihood of nanoparticle placement at the interface, resulting in the formation of aggregates within each of polymer phases. This phenomenon led to a significant increase in modulus and viscosity in low frequencies, as well as a rapid decrease in middle frequencies [25].

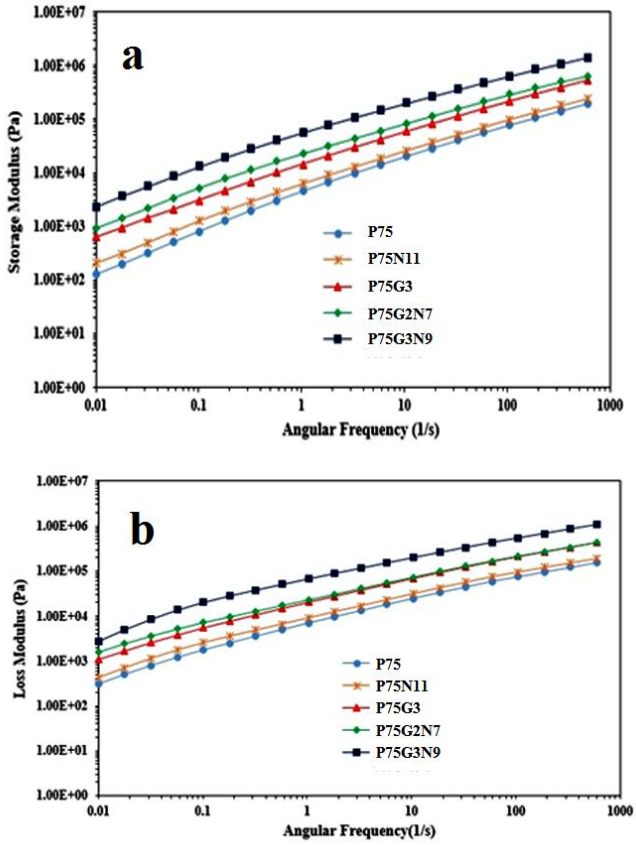

Figure 6: a) Storage modulus, and b) loss modulus, versus angular frequency for PLA/PCL blend and its compatibilized and uncompatibilized nanocomposites

The phase angle versus absolute value of complex modulus for the PLA/PCL compounds with varying GMA and NCC contents is depicted in Figure 7 using van Gurp-Palmen curves [26]. A phase angle close to 90° in the homogeneous state suggests liquid-like behavior, while a decrease in phase angle with increasing NCC and GMA contents at low G* values indicates enhanced elastic behavior. This analysis can aid in determining the rheological percolation threshold of the nanocomposite, which can be identified by a significant decrease in phase angle in the van Gurp-Palmen diagram, signaling a transition from liquid to solid behavior [27]. The van Gurp-Palmen plots demonstrate that the rheological percolation threshold of the PLA/PCL compounds falls within the range of 0.5 to 1 weight fraction.

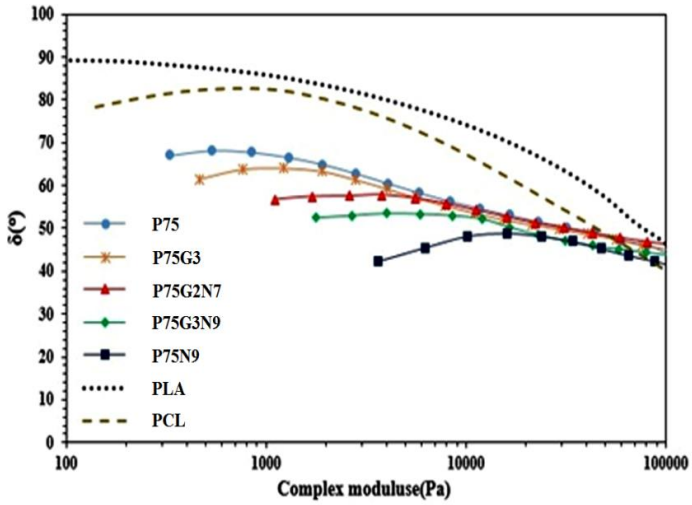

Figure 7: Van Gurp–Palmen plots for PLA/PCL blend and its compounds

Dynamic Mechanical Analysis

In order to analyze quantitatively the changes in nanoparticle distribution and size within the samples before and after the introduction of the compatibilizer, dynamic-mechanical properties testing was conducted. The results indicated that the nanocomposite with the added GMA exhibited a higher modulus compared to the uncompatibilized sample (Figure 8a), primarily attributed to the presence of large calcium NCC aggregates. However, at elevated temperatures, these aggregates and irregular nanoparticle structures experienced abrupt failure leading to a significant decrease in dynamic modulus [28].

Furthermore, the data depicted in Figure 8b illustrates that the addition of the compatibilizer resulted in a 50% reduction in the area under the loss diagram. This reduction can be ascribed to the rigid nature of the nanoparticle aggregates and chains with limited mobility on the nanoparticle surface, as well as entrapment between the aggregates (secluded area) [29].

Additionally, the nanoparticle dimensions were assessed through DLS, revealing that particles in the compatibilized sample had an average size of 170 micrometers, significantly larger than those in the uncompatibilized nanocomposite (Figure 8c). This increase in particle size was attributed to agglomeration, surface adsorption of polymer chains, and the presence of immobilized chains between the agglomerates, ultimately leading to property deterioration [30].

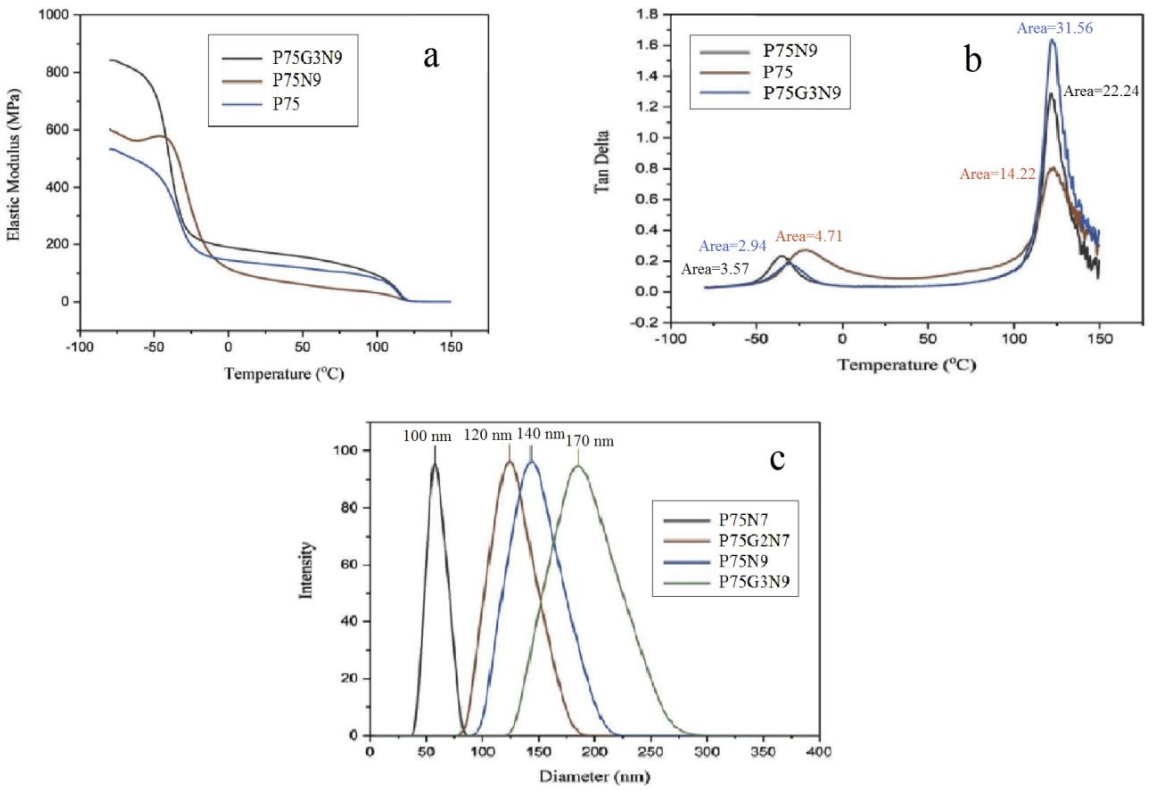

Figure 8: DMA plots: a) Elastic modulus vs. temperature, b) tan delta vs. temperature, and c) DLS plots for compatibilized and uncompatibilized nanocomposites and PLA/PCL blend

Conclusions

This study involved the preparation of various compositions of PLA/PCL blends with GMA as a chain extender, as well as PLA/PCL/NCC nanocomposites with 2 and 3 phr of GMA. The findings indicate that the inclusion of GMA significantly enhances the elongation at break of PLA, increasing it from 10% to approximately 180%. Moreover, all compatibilized PLA/PCL

blends exhibit lower permeability compared to compatibilized PLA, demonstrating that the addition of PCL reduces the oxygen permeability of PLA. The enhanced barrier properties observed in PLA/PCL samples are attributed not only to the intrinsic barrier properties of PCL but also to the promotion of crystallinity in PLA. Furthermore, the introduction of NCC results in a decrease in tensile properties. The compatibilized nanocomposite samples with 75 wt. % PCL and NCC particles exhibit lower tensile properties and oxygen permeability. The incorporation of 7 and 9 phr NCC leads to a decrease in barrier properties due to nanoparticle aggregation, which differs from the incompatibilized PLA/PCL nanocomposite. It is noted that the strengthening of the polymer interface by GMA and the tendency of NCC particles to be in the polymer phases rather than being localized at the interface contribute to these outcomes. Ultimately, the reduction in barrier properties may be attributed to phase separation of the blend components.

Declaration of Conflicting Interests

The author(s) declared no potential conflicts of interest with respect to the research, authorship, and/ or publication of this article.

Funding

The author(s) received no financial support for the research, authorship, and/or publication of this article.

Data Availability Statement

Data is available within the article and can be available on request.

References

1. MP Arrieta, E Fortunati, F Dominici, J López, JM Kenny (2015) Bionanocomposite films based on plasticized PLA – PCL / cellulose nanocrystal blends, Carbohydr. Polym, 121: 265–75.

2. H Gao, J Li, Z Li, Y Li, X Wang et al. (2023) Enhancing interfacial interaction of immiscible PCL/PLA blends by in-situ cross-linking to improve the foamability, Polym. Test, 124: 1-10.

3. S Huang, H Wang, W Ahmad, A Ahmad, NI Vatin et al. (2022) Plastic Waste Management Strategies and Their Environmental Aspects: A Scientometric Analysis and Comprehensive Review," Int. J. Environ. Res. Public Health, 19: 8.

4. R Banerjee, SS Ray (2021) An overview of the recent advances in polylactide-based sustainable nanocomposites," Polym. Eng. Sci, 61: 617–49.

5. G Ye, Z Li, B Chen, X Bai, X Chen et al. (2022) Performance of polylactic acid/polycaprolactone/microcrystalline cellulose biocomposites with different filler contents and maleic anhydride compatibilization," Polym. Compos, 43: 5179–88.

6. E Özen Öner, ME Pekdemir, E Ercan, Y Say, M Kök et al. (2022) Novel of (PLA/PCL blend)/Gd2O3 rare earth oxide nanocomposites: Shape memory effect, thermal, magnetic, and mechanical properties, Polym. Compos, 43: 3096-103.

7. T Casalini, F Rossi, A Castrovinci, G Perale (2019) A Perspective on Polylactic Acid-Based Polymers Use for Nanoparticles Synthesis and Applications, Front. Bioeng. Biotechnol, 7: 1–16.

8. MD Sanchez-Garcia, E Gimenez, JM Lagaron (2007) Novel PET Nanocomposites of Interest in Food Packaging Applications and Comparative Barrier Performance With Biopolyester Nanocomposites," J. Plast. Film Sheeting, 23: 33-49.

9. JM Lagaron, E Núñez (2012) Nanocomposites of moisture-sensitive polymers and biopolymers with enhanced performance for flexible packaging applications, J Plast Film Sheeting, 28: 79-89.

10. R. Al-Itry, K Lamnawar, A Maazouz (2012) Improvement of thermal stability, rheological and mechanical properties of PLA, PBAT and their blends by reactive extrusion with functionalized epoxy, Polym. Degrad, 97: 1898-914.

11. G Li, M Zhao, F Xu, B Yang, X Li et al. (2021) Synthesis and Biological Application of Polylactic Acid," Molecules, 25: 5023–41.

12. MA Abdelwahab, A Flynn, B Chiou, S Imam, W Orts, E Chiellini (2012) Thermal , mechanical and morphological characterization of plasticized PLA e PCL blends," Polym. Degrad Stab J, 97: 1822-8.

13. K Hamad, M Kaseem, M Ayyoob, J Joo, F Deri (2018) Polylactic acid blends: The future of green, light and tough, Prog. Polym. Sci, 85: 83-127.

14. S Su, R Kopitzky, S Tolga, S Kabasci (2019) Polylactide (PLA) and Its Blends with Poly(butylene succinate (PBS): A Brief Review," Polymers (Basel), 1-21.

15. M Mehrabi Mazidi, A Edalat, R Berahman, FS Hosseini (2018) Highly-Toughened Polylactide- (PLA-) Based Ternary Blends with Significantly Enhanced Glass Transition and Melt Strength: Tailoring the Interfacial Interactions, Phase Morphology, and Performance," Macromolecules, 51: 4298–314.

16. K Hamad, M Kaseem, HW Yang, F Deri, YG Ko (2015) Properties and medical applications of polylactic acid : A review," Express polyme Lett, 9: 435-55.

17. G Maglio, A Migliozzi, R Palumbo, B Immirzi, MG Volpe et al. (1999) Compatibilized poly (e -caprolactone)/ poly (L -lactide) blends for biomedical uses, Macromol, 238: 236–8.

18. I Ferrer, A Manresa, JA Méndez, M Delgado-Aguilar, ML Garcia-Romeu (2021) Manufacturing PLA/PCL blends by ultrasonic molding technology," Polymers (Basel), 13: 1-17.

19. MP Arrieta, MD Samper (2014) Combined Effect of Poly (hydroxybutyrate) and Plasticizers on Polylactic acid Properties for Film Intended for Food Packaging, Polym Env, 25: 1–11.

20. V Sridhar, I Lee, HH Chun, H Park (2013) Graphene reinforced biodegradable poly(3-hydroxybutyrate-co-4-hydroxybutyrate) nano-composites," Express Polym. Lett, 7: 320-8.

21. M Zhang, NL Thomas (2010) Blending Polylactic Acid with Polyhydroxybutyrate : The Effect on Thermal , Mechanical , and Biodegradation Properties, Adv Polym Technol, 30: 67-79.

22. R Plavec, S Hlaváčiková, L Omaníková, J Feranc, Z Vanovčanová, K Tomanová et al. (2020) Recycling possibilities of bioplastics based on PLA/PCL blends, Polym Test, 92: 1–12.

23. AM El-hadi (2021) Effect of Processing Conditions on the Development of Morphological Features of Banded or Nonbanded Spherulites of Poly (3-hydroxybutyrate) (PCL) and Polylactic Acid (PLLA) Blends," Polym. Eng. Sci, 21: 2191–3.

24. A D'Anna, R Arrigo, A Frache (2019) PLA/PCL blends: Biocompatibilizer effects," Polymers (Basel), 11: 1416–28.

25. H Liu, J Zhang (2011) Research Progress in Toughening Modification of Poly (lactic acid)," Polyme Phys, 1051-83.

26. N Bumbudsanpharoke, S Ko (2015) Nano-Food Packaging : An Overview of Market , Migration Research , and Safety Regulations," Food Sci, 80: 910-23.

27. M Negaresh, A Javadi, H Garmabi (2024) Poly(lactic acid)/ poly(ε-caprolactone) blends: Separate effects of nanocalcium carbonate and glycidyl methacrylate on interfacial characteristics, J Thermoplast. Compos. Mater, 1–29.

28. Z.Duan (2013) Water vapour permeability of poly (lactic acid) nanocomposites, Membrane Science, 0–18.

29. TP Mohan, K Devchand, K Kanny (2016) Barrier and biodegradable properties of corn starch-derived biopolymer film filled with nanoclay fillers, J Plast Film Sheeting, 0: 1–28.

30. M Bartel, H Remde, A Bohn, J Ganster (2016) Barrier properties of poly (lactic acid)/ cloisite 30B composites and their relation between oxygen permeability and relative humidity, Appl Polym Sci, 44424: 1–10.